Kidney International, Vol. 66 (2004), pp. 1785–1793

Expression of somatostatin in the adult and developing mouse kidney

CARLTON M. BATES, HEATHER KEGG, and SANDY GRADY

Center for Human and Molecular Genetics, Children's Research Institute, Columbus, Ohio; and Division of Nephrology, Department of Pediatrics, College of Medicine & Public Health, The Ohio State University, Columbus, Ohio

Expression of somatostatin in the adult and developing mouse kidney.

Background. Somatostatin (somatotropin release inhibiting factor) (SRIF) has potent antiproliferative and antisecretory actions. In the adult kidney, somatostatin alters renal blood flow, ion transport, and water permeability. While some evidence suggests that SRIF may be produced by adult kidney tubular cells, the specific tubules generating SRIF are unknown. Somatostatin has also been detected in a variety of embryonic tissues, although it has not been described in the developing kidney. Our objective was to determine the expression pattern of SRIF in both the adult and embryonic mouse kidney.

Methods. We performed reverse transcriptase-polymerase chain reaction (RT-PCR) and immunofluorescence for SRIF in developing and adult mouse kidney tissues. We localized SRIF by dual or serial labeling immunofluorescence with specific markers.

Results. Somatostatin mRNA was present in kidneys throughout embryogenesis and into adulthood. Starting at embryonic day (E) 12.5, SRIF was strongly expressed at the interface of the metanephric mesenchymal cells and the basolateral surfaces of ureteric bud trunks. Starting at E16.5, the staining at the interface was confined to the peripheral ureteric bud trunks and the clefts of newly dividing ureteric bud ampullae. In older embryos, SRIF also appeared in medullary tubules that appeared to be maturing thin descending limbs of Henle. In the adult kidney, SRIF proteins localized exclusively to medullary thin descending limbs of the Henle loop.

Conclusion. In embryonic kidneys, SRIF is expressed first at the interface of the metanephric mesenchyme and basolateral ureteric bud and later in maturing thin descending limbs of Henle. Expression in the thin descending limb persists in the adult kidney.

Somatostatin, a 14 or a 28 amino acid peptide, is generated by sequential cleavage of N-terminal amino acids from a pre-pro and then a pro-peptide [1]. Somatostatin is highly conserved with 97% amino acid identity between human and rodent pre-pro peptides and 100% identity between human and rodent 14 and 28 amino acid peptides [1]. Somatotropin release inhibiting factor (SRIF) signaling is mediated via five different G-protein–coupled receptors, somatostatin receptors (SSTRs) 1 to 5 [1]. Somatostatin acts in the brain as a neurotransmitter and in a variety of primary and neoplastic tissues as an inhibitor of cell proliferation and/or an inhibitor of cell secretion [1]. In the adult metanephric kidney, somatostatin alters glomerular filtration and renal blood flow [2–4], inhibits tubular phosphate transport [2, 3, 5], and alters urine volume and free-water clearance [5–7].

In addition to having actions in the adult kidney, somatostatin appears to be produced in the kidney; however, the specific renal cells that generate somatostatin have either not been identified and/or may vary by species. Primary human glomerular mesangial cell cultures were reported to express somatostatin mRNA and to secrete the peptide into the media [8]. In rats, however, SRIF immunostaining was described in isolated glomerular cells that were clearly not mesangial cells (and in only one out of every five to ten glomeruli per 4 μm section) [9]. Heterogeneous mixtures of primary human renal tubular cells have also been reported to express somatostatin mRNA and to secrete the peptide into the media, but the specific tubular cells generating somatostatin were not identified [10].

Unlike the adult kidney, somatostatin expression has never been described in the developing kidney. Metanephric kidney development in the mouse begins at gestational day 11.5 (of a 19-day gestational period) when an evagination of the caudal nephric duct, the ureteric bud, contacts adjacent paired densities of mesodermal tissue, called the metanephric mesenchyme [11]. The mesenchyme stimulates the ureteric bud to repeatedly form ampullae that separate into two tips, which eventually elongate into new trunks [11]. In turn, each ureteric bud tip induces local areas of mesenchyme to convert into nephron epithelia [11]. As development proceeds,

Key words: somatostatin, embryonic kidney, adult kidney, immunohistochemistry.

Received for publication October 15, 2003
and in revised form March 29, 2004, and May 6, 2004
Accepted for publication May 18, 2004

maturing ureteric buds fuse with the nephrons and form the collecting ducts [11].

The purpose of our study was to describe the expression of somatostatin in the adult and developing mouse kidney. By reverse transcription-polymerase chain reaction (RT-PCR) followed by Southern blotting, we detected mRNA for somatostatin in mouse kidneys starting in young embryos and persisting into adulthood. In early embryonic kidneys, we detected strong somatostatin labeling at the interface of the metanephric mesenchyme and the basolateral surfaces of central ureteric bud trunks. In more mature embryos, the interface staining was confined to outer cortical regions around peripheral ureteric bud trunks and in clefts of ureteric bud ampullae as they began to divide. In older embryos, somatostatin also appeared in maturing medullary tubules that expressed markers consistent with thin descending limbs of Henle. In the adult kidney, somatostatin immunostaining was exclusively in medullary thin descending limbs of the Henle loop.

METHODS

RT-PCR and Southern blotting

The procedures used were outlined in detail previously [12]. Briefly, brains from 2- to 4-month-old CD-1 mice and kidneys from embryonic day (E) 12.5, E14.5, E16.5, E18.5, postnatal day (P) 14, and 2- to 4-month-old CD-1 mice were homogenized in Trizol (Invitrogen, Carlsbad, CA, USA). After addition of chloroform, the RNA was precipitated and resuspended in diethylpyrocarbonate-treated (DEPC) water. Any contaminating genomic DNA was digested with RNAse free RQ1 DNAse (Promega, Madison, WI, USA). The RNA was again precipitated and resuspended in DEPC water.

RT-PCR was performed at least three times for each sample. Kidney and brain total RNA samples were reverse transcribed with Moloney-murine leukemia virus (MMLV) Reverse Transcriptase (Promega) or had sterile water added as a negative control. The RT+, RT− and control genomic samples were then subjected to PCR amplification for both somatostatin and glyceraldehyde-3-phosphate dehydrogenase (GAPDH). The oligonucleotide primer sequences and the expected band sizes for each amplification are listed in Table 1. RT+, RT−, and genomic samples were amplified with *Taq* DNA polymerase (Invitrogen) for 35 total cycles for SRIF and for 25 cycles for GAPDH. The PCR products were electrophoresed on agarose gels with ethidium bromide.

To verify that the ethidium RT+ PCR bands represented amplified somatostatin cDNA, we performed Southern blotting. After depurination, denaturation, and neutralization, the DNA was then transferred by capillary action and crosslinked to Magna Nylon membranes (Micron Separations, Inc., Westboro, MA, USA). After prehybridization, the membranes were hybridized overnight with an [α-^{32}P]-adenosine triphosphate (ATP) (Amersham, Piscataway, NJ, USA) end-labeled dephosphorylated oligonucleotide (5′-GACCTCTGA TCCCTCTCCCCCAAACCCCATATCTCTTCCTTA-3′), whose sequence is contained within the PCR fragment. Probes against the ladder DNA were made by end labeling 25 ng of ladder itself. After washes, the membranes were exposed to x-ray film. Images were scanned and converted to Adobe Photoshop files.

Table 1. Polymerase chain reaction (PCR) primer constructs

Gene	Primer pairs	Size *bp*
SRIF	5′-GTCCTGGCTTT GGGCGGTGTCA-3′	383 (cDNA)
	3′-TAGAGAAGGAATT GAGGACCGGGG-5′	1048 (genomic)
GAPDH	5′-CTGACGTGCC GCCTGGAGAAA-3′	346
	3′-GATAGGGTTGAGCC GGGGGTTGT-5′	

Abbreviations are: SRIF, somatotropin release inhibiting factor; GAPDH, glyceraldehyde-3-phosphate dehydrogenase.

Animals and tissue sectioning for immunostaining

For the experiments in adult mice, at least three 2- to 4-month-old CD-1 female mice were used for each histologic experiment. Prior to the experiments, the mice were maintained on distilled water and standard mouse chow (Teklad Laboratories, Inc., Indianapolis, IN, USA). For each experiment, the mice were euthanized by CO_2 inhalation and then the brains and kidneys were removed. Each organ was divided once with a blade in the midline transverse plane and fixed in Histochoice (Amresco, Solon, OH, USA) for 4 to 6 hours. For the experiments in developing kidneys, pregnant CD-1 mice were euthanized as above and embryos at ages E12.5, E14.5, E16.5, and E18.5 were removed and placed directly in Histochoice fixative overnight. In addition to CD-1 mice, Hoxb7GFP transgenic mice that express green fluorescent protein (GFP) in ureteric bud tissues [13] (gift from Frank Costantini, Columbia University) were used for many of the embryonic experiments. P14 mice were also euthanized with CO_2 and their kidneys removed, divided, and fixed in the same manner as the adult kidneys.

In preparation for cryostat sectioning, all fixed tissues were transferred to 25% sucrose overnight at 4°C. Tissues were then frozen in 22-oxacalcitriol (OCT) embedding media (Sakura Finetek, Inc.) in crushed dry ice. The kidneys, brains, and embryos were then cryostat sectioned into 7 to 10 μm slices which were placed on charged glass microscope slides (Surgipath, Richmond, IL, USA).

Antibodies used for immunofluorescence

SRIF immunostaining in all tissues was performed with a rabbit polyclonal antibody against the bioactive 14 amino acid peptide at a 1:500 dilution (Bachem, San Carlos, CA, USA). This antibody has been used previously

for somatostatin immunostaining in rat neurons [14]. A second rabbit polyclonal antibody against the 14 amino acid peptide was used for to confirm the immunostaining pattern in adult mouse kidneys and brains at a 1:20 dilution (Abcam, Cambridge, MA, USA). To further test the specificity of the SRIF antisera, the 14 amino acid somatostatin peptide (Bachem), the 14 amino acid cortistatin peptide (American Peptide Company, Sunnyvale, CA, USA), and urotensin II (American Peptide Company) were used for blocking experiments at 10 μg/mL.

For localization studies in developing kidneys, rabbit polyclonal antibodies against aquaporin 1 (AQP-1) (Alpha Diagnostic, San Antonio, TX, USA) were used at concentrations of 20 μg/mL to label proximal tubules in the cortex and thin descending limbs of the loop of Henle in the medulla [15]. Polyclonal antibodies against Golgi (Affinity BioReagents, Golden, CO, USA) were used at 1:1000. In addition, a mouse monoclonal antibody against pan cytokeratins (Sigma Chemical Co., St. Louis, MO, USA) was used at a 1:8 dilution to identify ureteric bud epithelia [16]. In the Hoxb7GFP transgenic mice, a rabbit polyclonal antibody against GFP (Molecular Probes, Eugene, OR, USA) was used at a 1:500 dilution to identify ureteric bud epithelia.

For localizing studies in the adult kidneys, rabbit polyclonal antibodies against AQP-1, aquaporin-2 (AQP-2) (Calbiochem, San Diego, CA, USA), and Tamm-Horsfall protein (THP) (Biomed Technologies, Lake Hopatcong, NJ, USA) were used at concentrations of 20 μg/mL, 1:100, and 1:500, respectively. AQP-2 is a specific marker for the principal cells of the cortical collecting tubules and cortical and medullary collecting ducts [15]. THP is a specific marker for the cortical and medullary thick ascending limbs of the loop of Henle [17].

Secondary antibodies included goat antirabbit cyanine (Cy)2 conjugates, antirabbit Cy3 conjugates, antirabbit Cy3 FAB fragments, and antimouse Cy2 conjugates used at 1:20, 1:500, 1:500, and 1:20, respectively (Jackson Immunochemicals, West Grove, PA, USA).

Immunofluorescence

As described previously [12], the tissues were incubated overnight at 4°C with anti-SRIF or anti-Golgi antisera alone, with SRIF antisera and blocking peptide (preincubated at room temperature for 2 hours), or with SRIF antisera and pan cytokeratin antibodies. The tissues were then incubated with antirabbit Cy3-conjugated antibodies (for the Golgi and most of the SRIF single labeling) or with the antirabbit antibodies and antimouse Cy2 conjugates (for the pan cytokeratin antisera). For the SRIF and Golgi labeling in serial sections, Cy2 conjugates were used to detect SRIF. For the adult kidney dual-labeling studies, the localizing antirabbit antibodies (i.e., AQP-1, AQP-2, and THP antibodies) were applied first, followed by secondary monovalent Cy3-conjugated FAB fragments that "converted" each localizing antibody to a different species [18]. The SRIF antibody was then used as the second primary antibody, followed by antirabbit Cy2-conjugated secondary antibodies. For the remaining dual-labeling studies, SRIF antisera were used as the first primary antibody (labeled with FAB Cy3 fragments) and the localizing antibodies (AQP-1 and GFP antibodies) were used as the second primary antibody (labeled with Cy2). To control for the possibility of the second antirabbit secondary antibody cross-reacting with the first primary antibody, tissues incubated with the first primary antibody and antirabbit Cy3-conjugated FAB fragments were compared with adjacent tissues incubated with the first primary, the Cy3 FAB secondary and the second Cy2-conjugated secondary antibody.

Imaging

Images were captured with a MagnaFire digital camera (Optronics, Goleta, CA, USA) mounted on a DM LB microscope (Leica, Bannockburn, IL, USA). Files were then converted to Adobe Photoshop format. Fluorescent images from dual-labeled slides were superimposed to generate merged images.

RESULTS

To determine if somatostatin mRNA transcripts were expressed in the mouse kidney, we performed RT-PCR followed by Southern blotting. We detected PCR bands of the appropriate size for somatostatin cDNA in adult kidney and brain samples that were reverse transcribed (RT+) and not in control samples without reverse transcriptase (RT−) (Fig. 1A, middle panel). Likewise, we observed bands consistent with somatostatin cDNA in RT+ embryonic (E12.5, E14.5, E16.5, and E18.5) and postnatal (P14) mouse kidney samples and not in RT− tissues (Fig. 1B, top panel). As expected, PCR on genomic DNA (G) resulted in bands of approximately 1000 bp (Fig. 1A, middle panel and B, top panel), proving that the smaller bands in the RT+ samples were not from contaminating genomic DNA. PCR for GAPDH in the linear range also revealed bands of the expected size and of relatively equal intensity in all RT+ samples (not shown). We transferred all of the PCR products to nylon membranes and performed Southern blotting with oligonucleotide probes against portions of somatostatin cDNA expected to be amplified by the PCR primers. We detected bands only in the RT+ adult kidney and brain samples (Fig. 1A, right panel), the RT+ developing kidney samples (Fig. 1B, bottom panel), and genomic samples (Fig. 1). Furthermore, the Southern bands clearly aligned with the PCR ethidium bands (Fig. 1). Thus, we concluded that mRNA for somatostatin is expressed in both the adult and developing mouse kidney.

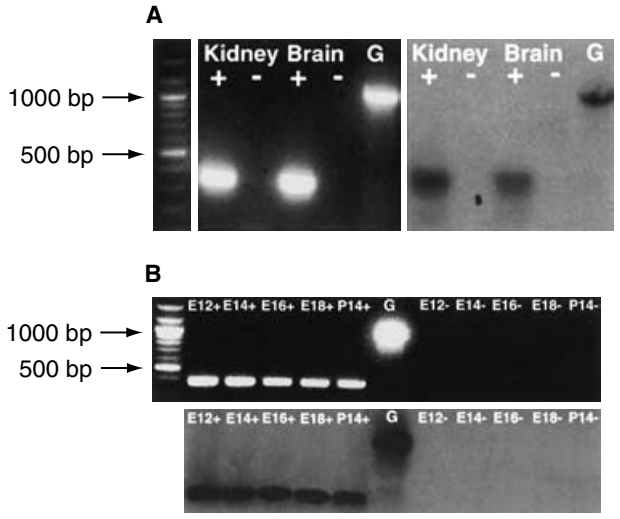

Fig. 1. Reverse transcription-polymerase chain reaction (RT-PCR) and Southern blotting for somatostatin. (*A*) Compared with a 100 bp ladder (right panel), PCR ethidium bands of the appropriate size for somatotropin release inhibiting factor (SRIF) cDNA are present in kidney and brain RNA samples with RT added (+) but not in kidney and brain samples when no RT was added (−) (middle panel). PCR on genomic DNA (G) reveals a band of approximately 1000 bp as expected (middle panel). Autoradiographs of Southern blots with specific probes against SRIF confirm that the ethidium bands in the RT+ and genomic samples represent amplified cDNA and genomic DNA, respectively (right panel). (*B*) PCR bands of the appropriate size for SRIF cDNA are also present in embryonic (E) E12.5, 14.5, 16.5, 18.5, and postnatal (P) P14 mouse kidney RNA when RT was added but not without RT (−) (top panel). Southern blots against SRIF again confirm that the PCR bands represent cDNA and genomic DNA, respectively (lower panel).

We then performed immunofluorescence with somatostatin antiserum to determine SRIF protein expression in renal tissues. In young embryonic kidneys, we observed labeling at the interface of the metanephric mesenchyme and basolateral surfaces of branching epithelium consistent with ureteric bud tissue (Fig. 2A, arrows). In the medulla of older embryonic kidneys, we also observed SRIF staining, suggestive of tubules (Fig. 2C, arrow). In adult mouse kidneys, we observed widespread somatostatin staining in medullary epithelial tubules (Fig. 2E, arrow) and not in the cortex (not shown). To test the specificity of the antisera, we performed immunofluorescence in adult mouse brain tissues and observed staining of neurons in the fourth layer of the cerebral cortex (Cor) and the hippocampus (Hc) (Fig. 2K, arrows) as expected [1]. We also preincubated the antisera with somatostatin-14 (the immunizing peptide) and completely blocked the staining in all kidney and brain sections (Fig. 2B, D, F, and L, arrowheads). In adult kidney sections, we also preincubated the SRIF antisera with cortistatin and urotensin II (somatostatin-related peptides [19]), but found no decrease in signal compared with anti-SRIF antisera alone (Fig. 2G to J). Thus, we concluded that somatostatin protein is expressed in both developing and adult mouse kidneys.

To further characterize the expression of somatostatin in young embryos, we first utilized Hoxb7GFP transgenic mice that express GFP in the ureteric bud. Since the fixative we used on the tissues quenched most of the GFP fluorescence, we performed dual-labeling immunofluorescence with somatostatin antisera (red) and anti-GFP antibodies (green). In every embryonic kidney we tested, epithelia with adjacent SRIF staining (Fig. 3A, arrow) also expressed GFP (Fig. 3B) as observed clearly on merged images (Fig. 3C). Control experiments with SRIF antiserum followed by antirabbit Cy3 FAB antibody fragments (Fig. 3D) and SRIF antiserum followed by Cy3 FAB fragments and then antirabbit Cy2 antibodies (Fig. 3F) all demonstrated staining at/near basolateral surfaces on red filters (arrowheads). When we overexposed the green filters, both the SRIF/FAB Cy3 (Fig. 3E) and the SRIF/FAB Cy3/Cy2 (Fig. 3G) images revealed minor spectral overlap (arrowheads) and some persistent direct fluorescence from the GFP, but no apparent cross-reactivity of the Cy2 secondary with SRIF antibody/FAB Cy3 complexes. To then determine whether the ureteric bud was likely secreting SRIF at its basolateral surface, we performed staining for somatostatin and Golgi apparatus on several adjacent serial sections of wild type E14.5 kidneys. While somatostatin was present at/near the ureteric bud basolateral surface as expected, (Fig. 3H, concave arrow) ureteric bud staining for the Golgi apparatus appeared at the lumenal surface (Fig. 3I, concave arrowhead), suggesting that SRIF was not being secreted by the ureteric bud [the other Golgi-positive signal is present in the surrounding mesenchyme (Fig. 3I)]. Thus, we concluded that in young embryos, somatostatin was present at the interface of the metanephric mesenchyme and the basolateral surface of ureteric bud epithelia.

To characterize the timing and pattern of somatostatin expression along the basolateral ureteric bud, we examined several Hoxb7GFP embryonic and postnatal kidney sections dual-labeled for SRIF (red) and either GFP or pan-cytokeratin (green) to label the ureteric bud epithelia (Fig. 4). In cross-sections of E12.5 kidneys, we observed SRIF staining around the main central ureteric bud trunk (Fig. 4A, arrow) and around the first two branches from the main trunk (Fig. 4B, arrows). In longitudinal sections capturing the first two and subsequent branches of the ureteric bud, we detected SRIF labeling around the trunks (Fig. 4C, arrows) but not at outer bud tips (Fig. 4C, arrowheads). By E14.5, SRIF expression persisted along many early ureteric bud trunks (Fig. 2A). In addition, as new ureteric bud ampullae just began dividing (Fig. 4D), we observed somatostatin expression at/near the midline clefts (arrow) but not at the early tips (arrowheads). As the ampullae continued to divide, SRIF staining persisted along the medial edges of the emerging ureteric bud trunks (Fig. 4E and F, arrows). By E16.5, SRIF expression continued at ampullary clefts

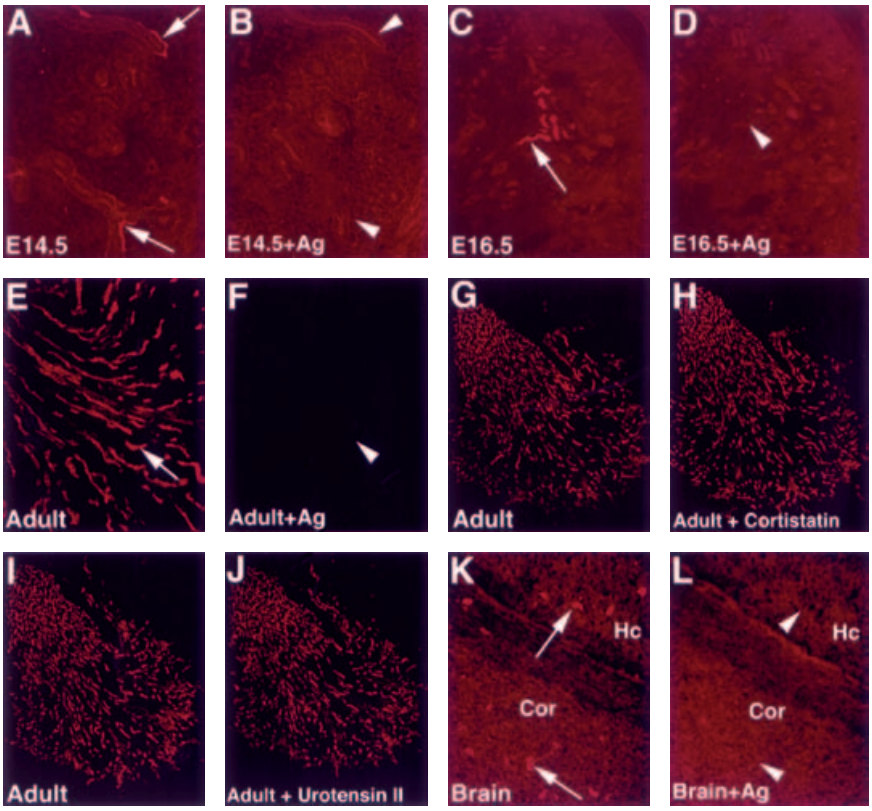

Fig. 2. Immunofluorescence for somatostatin (SRIF) with and without immunizing antigen in developing and adult mouse tissues. (*A* and *B*) Staining at/near basolateral tubular surfaces in embryonic (E) E14.5 kidneys (A, arrows) is blocked by immunizing antigen (B, arrowheads). (*C* and *D*) Cytoplasmic/lumenal tubular staining in E16.5 medulla (C, arrow) is blocked by immunizing antigen (D, arrowhead). (*E* and *F*) Adult kidney medullary staining (E, arrow) is blocked by preincubation with immunizing peptide (F, arrowhead). (*G* to *J*) Adult kidney medullary staining (G and I) is not blocked by preincubation with cortistatin (H) or urotensin II (J). (*K* and *L*) Staining in fourth layer of cerebral cortex (Cor) and hippocampus (Hc) (K, arrows) in brain is blocked by immunizing antigen (L, arrowheads) (A to D and K and L 200× magnification; E and F 100× magnification; G to J 40× magnification).

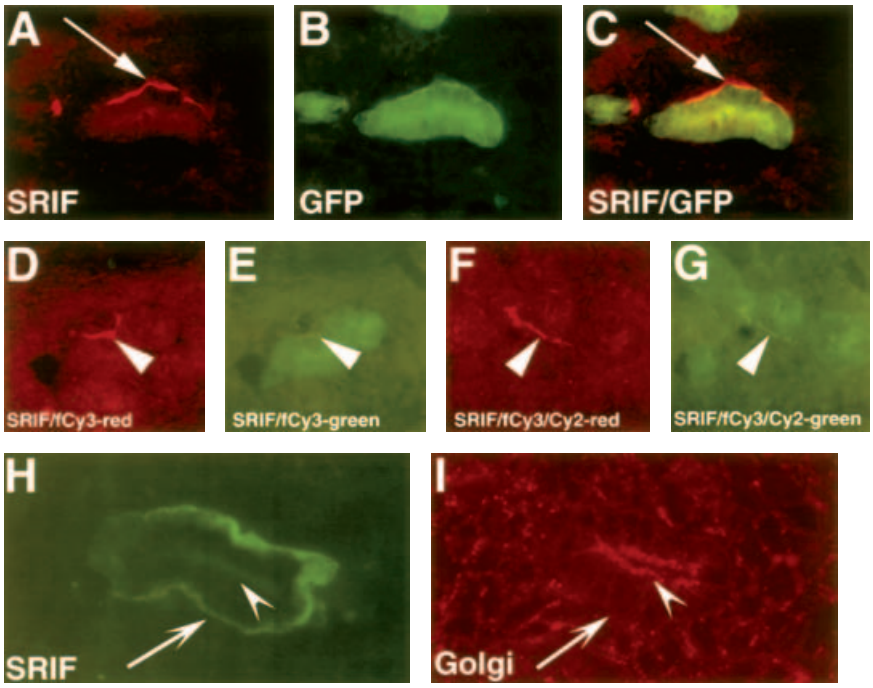

Fig. 3. Characterization of embryonic kidney epithelium with somatostatin (SRIF) immunofluorescence at/near its basolateral surface. (*A* to *C*) In HoxB7GFP transgenic mice, dual-labeled embryonic (E) E14.5 embryonic kidney epithelia with SRIF staining at/near its basolateral surfaces (A, red, arrow) and green fluorescent protein (GFP)-positive ureteric bud tissue (B, green) overlap on merged images (C). (*D* to *G*) Dual-labeling controls. SRIF antiserum followed by antirabbit cyanine (Cy) Cy3 FAB antibody fragments results in linear staining on red filters (D, arrowhead) and minor spectral overlap (and persistent direct fluorescence from the GFP) on overexposed green filters (E). Addition of Cy2-conjugated antirabbit antibodies (used to label the GFP antibody) resulted in similar staining on both the red filters (F) and the green filters (G). (*H* and *I*) In adjacent sections of wild-type E14.5 mice, SRIF labeling is along the basolateral surface of the ureteric bud (H, concave arrow), whereas Golgi apparatus staining is present at the lumenal surface of the ureteric bud (I, concave arrowhead) (200× magnification).

and along medial basolateral edges of emerging cortical ureteric bud trunks (Fig. 4G to I); however, SRIF staining at/near the basolateral ureteric bud was absent in the maturing medulla (see Fig. 5). By E18.5, SRIF staining at/near basolateral epithelial surfaces was present only along immature ureteric bud tissues at the outer cortex in the same pattern as younger embryos (Fig. 4J). By P14, when all ureteric bud branching had ceased, we did not detect any somatostatin immunostaining at basolateral epithelia in the cortex (Fig. 5G). Thus, we concluded that

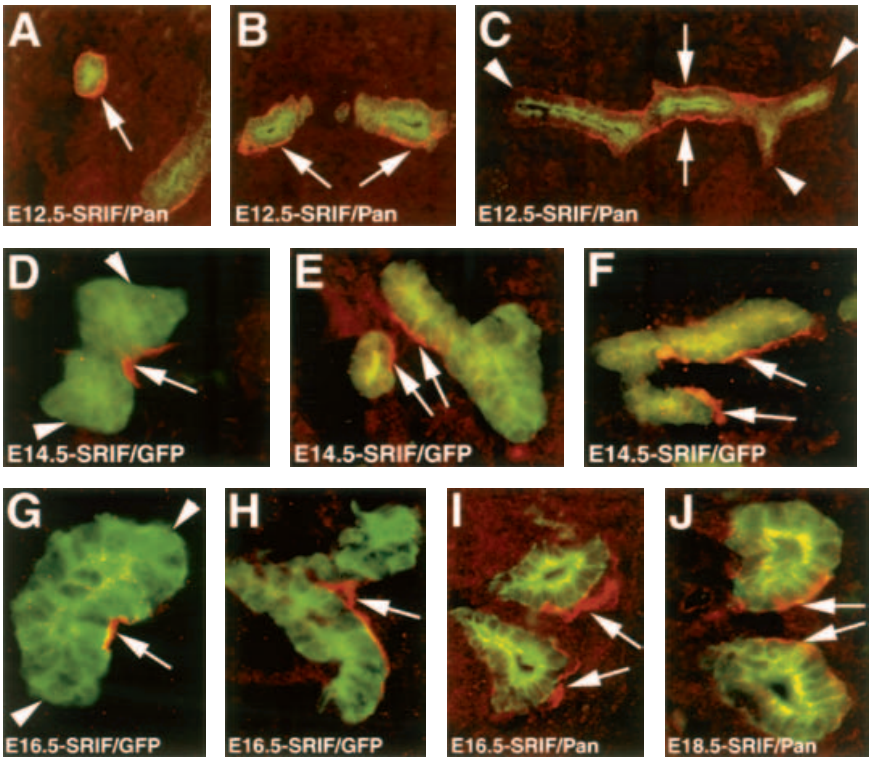

Fig. 4. Merged immunofluorescent images of somatostatin (SRIF) (red) and markers of the ureteric bud (green) in embryonic kidneys of different ages. (*A* and *B*) Cross-sections of embryonic (E) E12.5 kidneys show SRIF staining around the main central ureteric bud trunk (A, arrow) and the first two branches (B, arrows). (*C*) Longitudinal sections of E12.5 kidneys reveal SRIF labeling around trunks (arrows) but not outer tips (arrowheads) of the first two and subsequent ureteric bud branches. (*D*) E14.5 kidneys show SRIF expression at/near midline clefts of dividing ureteric bud ampullae (arrow) and not at the early tips (arrowheads). (*E* and *F*) E14.5 kidneys demonstrate persistent SRIF staining along medial edges of emerging ureteric bud trunks as ampullae continue to divide (arrows). (*G* to *I*) E16.5 kidneys show SRIF expression at new ampullary clefts (G, arrow) and along medial edges of emerging cortical ureteric bud trunks (H and I, arrows), but not at outer tips (G, arrowhead). (*J*) E18.5 kidneys demonstrate SRIF staining around basolateral surfaces of ureteric bud epithelia (arrows) at the outer cortex with the same pattern as younger embryos (A to C 100× magnification; G to J 200× magnification). Abbreviations are: GFP, anti-green fluorescent protein; pan, anti-pan cytokeratin.

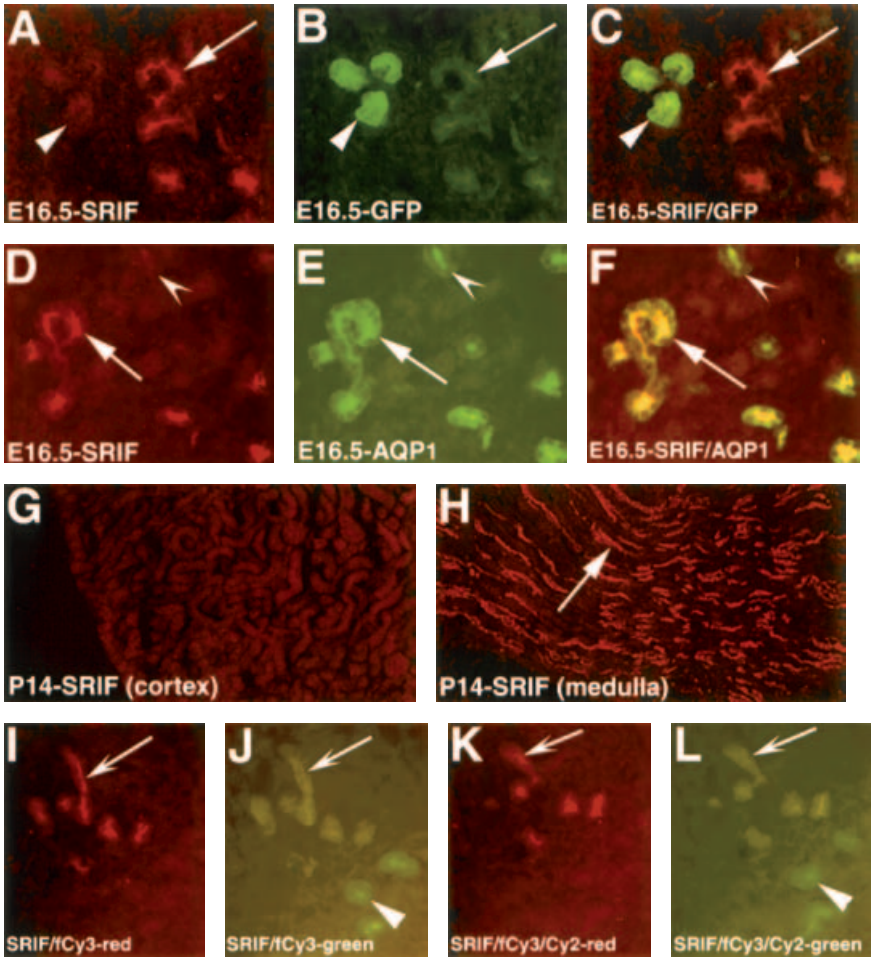

Fig. 5. Fluorescent micrograph showing localization of medullary lumenal somatostatin (SRIF) staining at E16.5 and persistence of medullary staining at postnatal (P) P14. (*A* to *C*) Embryonic (E) E16.5 kidney tubules with lumenal SRIF staining (A, red, arrow) and green fluorescent protein (GFP)-positive ureteric bud epithelia (B, green, arrowhead) do not overlap on merged images (C). (*D* to *F*) E16.5 kidney tubules with lumenal SRIF expression (D, arrow) always colabel with aquaporin-1 (AQP-1) (E, arrow) on merged images (F), although some AQP-1–positive tubules do not express SRIF (concave arrowheads). (*G* and *H*) At P14, SRIF labeling is now completely absent in the renal cortex (G), but persists in many medullary tubules (H, arrow). (*I* to *L*) Dual-labeling controls. SRIF antiserum followed by antirabbit cyanine (Cy) Cy3 FAB antibody fragments results in lumenal staining on red filters (I, concave arrow) and minor spectral overlap (and persistent direct fluorescence from the GFP) on overexposed green filters (J); addition of Cy2-conjugated antirabbit antibodies (used to label the GFP antibody) showed similar staining on both the red filters (K) and the green filters (L) (A to F and I to L 200× magnification; G and H 100× magnification).

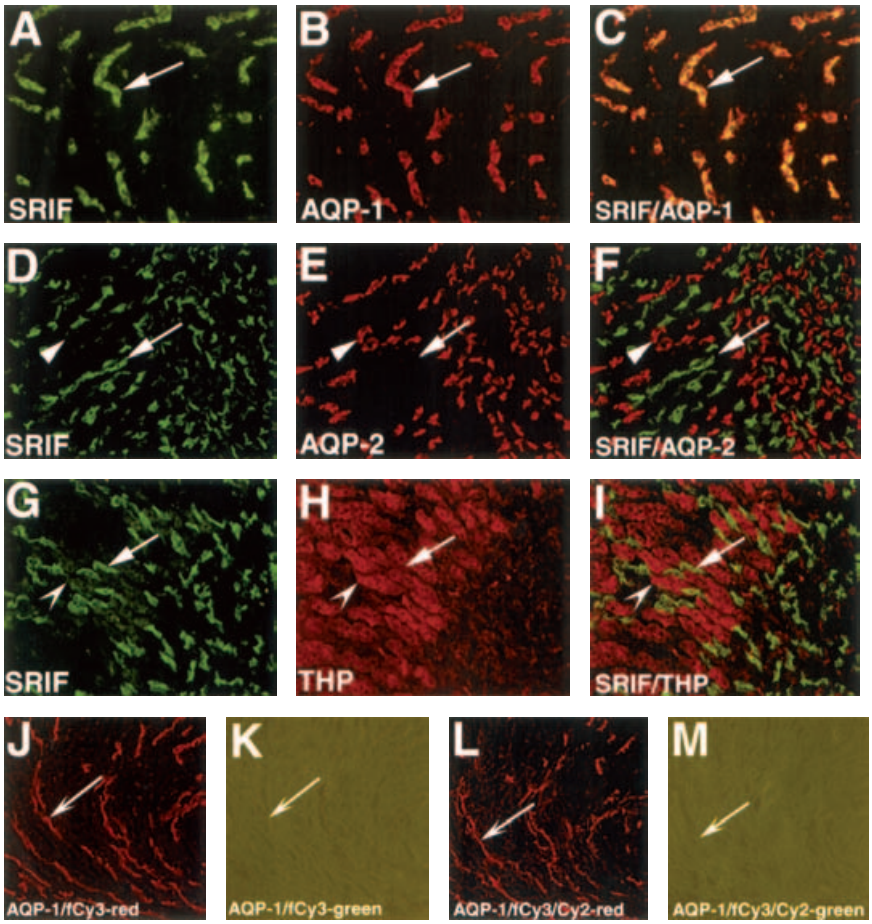

Fig. 6. Dual-labeling immunofluorescence of somatostatin (SRIF) (green) and localizing markers (red) in the adult kidney medulla. (*A* to *C*) SRIF (A, arrow) and aquaporin-1 (AQP-1) (B, green), a marker of the thin descending limb of Henle, completely overlap on merged images (C, arrow). (*D* to *F*) SRIF (D, arrow) and the collecting duct marker AQP-2 (E, arrowhead) are not coexpressed on merged images (F). (*G* to *I*) SRIF (G, arrow) and Tamm-Horsfall protein (THP) (H, concave arrowhead), a marker of the thick ascending limb of Henle, do not overlap on merged images (I). (*J* to *M*) Controls. AQP-1 antiserum followed by antirabbit FAB fragments with cyanine (Cy) Cy3 results in bright tubular cell staining (concave arrows) on red filters (J) and no spectral overlap on overexposed green filters (K); addition of Cy2-conjugated antirabbit antibodies (used to label the SRIF antibody) resulted in similar staining on red filters (L) and demonstrated no spectral overlap or cross reactivity with AQP-1/FAB Cy3 antibody complexes on overexposed green filters (M) (200× magnification).

somatostatin protein is first expressed at/near the basolateral surfaces of early main ureteric bud trunks and then at ampullary clefts and subsequent ureteric bud trunks, but never near ureteric bud tips.

In E16.5 kidneys, while SRIF staining at/near the basolateral ureteric bud surface was present only in the cortex, we observed lumenal somatostatin staining in medullary tubules (Fig. 5). To determine if these were also ureteric bud tissues, we performed dual labeling in Hoxb7 transgenic mice for somatostatin (Fig. 5A, arrow) and GFP (Fig. 5B, arrowhead), but observed no overlapping expression on merged images (Fig. 5C). To determine if the medullary tubules were maturing thin descending limbs of Henle, we then performed dual labeling for SRIF and AQP-1. We observed that every somatostatin positive tubule (Fig. 5D, arrow) also expressed AQP-1 (Fig. 5E, arrow) on merged images (Fig. 5F); however, a few AQP-1 positive tubules did not express somatostatin (concave arrowheads). By E18.5, lumenal SRIF staining was present on a large number of medullary tubules that all expressed AQP-1, although as in E16.5 kidneys, a small number of AQP-1–positive tubules did not express somatostatin (not shown). In P14 kidneys (when nephrogenesis was finished), somatostatin was present exclusively in medullary tubules (Fig. 5G and H). Control experiments with SRIF antiserum followed by antirabbit Cy3 FAB antibody fragments (Fig. 5I) and SRIF antiserum followed by Cy3 FAB fragments and then antirabbit Cy2 antibodies (Fig. 5K) all demonstrated luminal staining on red filters (concave arrows). When we overexposed the green filters, both the SRIF/FAB Cy3 (Fig. 5J) and the SRIF/FAB Cy3/Cy2 (Fig. 5L) images revealed minor spectral overlap (concave arrows) and some persistent direct fluorescence from the GFP (arrowheads), but no apparent cross-reactivity of the Cy2 secondary with SRIF antibody/FAB Cy3 complexes. Thus, we concluded that in older embryos and young postnatal mice, somatostatin is present in maturing medullary thin descending limbs of Henle.

To identify the medullary tubules expressing somatostatin protein in the adult kidney, we performed dual-labeling immunofluorescence with SRIF antiserum (green) and localizing markers (red) (Fig. 6). Somatostatin (Fig. 6A, arrow) and AQP-1 (Fig. 6B, arrow), a marker of thin descending limbs of the Henle loop, demonstrated complete overlapping expression

on merged images (Fig. 6C, arrow). In contrast, SRIF (Fig. 6D, arrow) did not colabel with AQP-2 (Fig. 6E, arrowhead) in the collecting duct on merged images (Fig. 6F). Somatostatin (Fig. 6G, arrow) was also not coexpressed with THP (Fig. 6H, concave arrowhead), a marker of the thick ascending limb of Henle, on merged images (Fig. 6I). Furthermore, unlike thick ascending limbs that are only present in the outer medulla, somatostatin-expressing tubules were located in both the inner and outer medulla (Fig. 6I). Control experiments demonstrated no spectral overlap of red anti-AQP-1/antirabbit FAB Cy3 antibody complexes (Fig. 6J) on overexposed green filters (Fig. 6K); addition of Cy2-conjugated antirabbit antibodies (used to label the SRIF antibody) resulted in similar staining on red filters (Fig. 6L) and demonstrated no spectral overlap or cross reactivity with AQP-1/FAB Cy3 antibody complexes on overexposed green filters (Fig. 6M). Thus, we concluded that the adult mouse kidney tubules expressing somatostatin protein were the medullary thin descending limbs of Henle.

DISCUSSION

In this study, we describe the presence of somatostatin mRNA and protein in both the adult and developing mouse kidney. The expression pattern of SRIF in the adult mouse kidney is surprisingly different than what was reported in the rat. Whereas we detected strong expression in mouse medullary thin descending limbs of Henle, no tubular expression was described in the rat [9]. One explanation could be that we fixed our mouse kidneys with Histochoice, while the other group used paraformaldehyde (PFA) to fix the rat kidneys [9]. Histochoice is an alcohol based fixative that has been shown to cause less cross-linking than PFA, often resulting in superior immunostaining signal strength [20]. As has happened with other antisera we have used for other studies, both SRIF antisera we utilized in this study did not give any specific immunostaining signal in PFA-fixed mouse kidneys (not shown). Why we did not detect the presence of somatostatin in mouse glomeruli, as was reported in the rat, is not as clear. The reported SRIF immunostaining in rat kidneys was very sparse (only one out of every five to ten glomeruli) and in unidentified cells that were not thought to be any of the usual cells known to populate glomeruli (i.e., epithelial cells, endothelial cells, or mesangial cells) [9]. Despite using two different antibodies against SRIF, we did not find expression in such cells in the mouse (although the tubular staining was the same with both antibodies).

While the reported staining pattern for somatostatin in rat kidneys contrasted greatly with the expression profile in human kidney cells, there were some similarities between what we found in mice and what was found in humans. Heterogeneous mixtures of cultured human tubular cells expressed somatostatin mRNA by both RT-PCR and Northern blotting and were capable of secreting the peptide into the media [10]. The particular cells that constituted the cultures were not identified with molecular markers, and thus may have included thin descending limbs of Henle that were expressing the peptide. In a separate report, human mesangial cell cultures expressed somatostatin mRNA by RT-PCR and secreted the peptide into media [8], while as noted above, we found no SRIF staining in mouse glomeruli. Although somatostatin expression patterns in humans and rodents are usually comparable, there are exceptions. For instance, SRIF mRNA is expressed in the granular cell layer of rat cerebellum, whereas it is not found in the human cerebellum [21]. Thus, the absence of somatostatin staining in mouse glomeruli (while it is present in human mesangial cells) may represent a species-related difference in SRIF expression patterns.

In addition to SRIF, we have we have previously found that somatostatin receptors are expressed in the adult mouse kidney (in glomeruli, proximal tubules, and collecting ducts) [12, 22]. This implied paracrine/autocrine signaling in the adult kidney has been described in many other organs such as the brain [21], the pancreas [1, 23], the retina [24], ovarian tumors [25], and neuroblastomas [26]. In the adult kidney, SRIF may be secreted by cells of the thin descending limb of Henle into the tubular lumen to bind its collecting duct receptors downstream; the peptide may also be secreted into the peritubular vasculature to be circulated back to its receptors in glomeruli and proximal tubules. Although no published data exist on somatostatin receptor expression in the embryonic kidney, in immature regions of the developing kidney, the local vasculature has not yet formed; thus, the peptide is likely produced locally. Furthermore, based of the localization data with Golgi markers, the cells producing somatostatin are unlikely to be ureteric bud cells.

While somatostatin has many actions in the adult kidney (see above), its presence in the developing kidney is a completely novel finding and its actions there are unknown. In other rapidly growing tissues, somatostatin has very potent antiproliferative effects. Somatostatin or its analogues blunt growth rates of human pituitary tumors, endocrine pancreatic tumors, mammary tumors, and carcinoids that express SSTRs [25, 27, 28]. Most of the T and B lymphocytes with somatostatin receptors proliferate less when treated with ligand [29]. Somatostatin or its analogues also dramatically reduce rates of proliferation in gut mucosal epithelium as measured in rabbit ileal organ cultures [30] and in rat intestines in vivo [31, 32]. Fetal cartilage and bone precursor cells also express SSTRs and display blunted growth rates after treatment with somatostatin [1]. In the developing kidney, the midline clefts of the ureteric bud ampullae and the emerging ureteric bud trunks do not proliferate as rapidly as the

expanding ureteric bud tips [11]. Perhaps SRIF acts on the former tissues or mesenchymal tissues to decrease proliferation rates as is necessary for the proper formation of the kidney. The identification of somatostatin receptors in the developing kidney would provide more evidence that SRIF is acting locally.

CONCLUSION

We have detected the expression of somatostatin mRNA in both developing and adult mouse kidneys. In developing kidneys, somatostatin first appears at the interface of the metanephric mesenchyme and the basolateral surfaces of the ureteric bud central trunks; later SRIF appears at/near the midline clefts of ureteric bud ampullae and on the medial surfaces of the emerging ureteric bud trunks. In older embryonic kidneys, somatostatin is expressed in maturing medullary tubules that label with markers of the thin descending limb of Henle. In adult kidneys, somatostatin proteins are exclusively expressed in medullary thin descending limbs of the Henle loop. Finally, the presence of somatostatin and its receptors in the adult mouse kidney implies paracrine/autocrine signaling.

ACKNOWLEDGMENTS

The authors wish to thank Dr. Martin Turman for advice and helpful discussions. This study was supported by grants from the National Institutes of Health, 5 P30 HD34615-02 and the American Society of Nephrology Carl W. Gottschalk Award (C.M.B.).

Reprint requests to Carl Bates, M.D., Section of Nephrology and Center for Cellular and Vascular Biology, Children's Research Institute, 700 Children's Drive, Columbus, Ohio 43205.
E-mail: batesc@pediatrics.ohio-state.edu

REFERENCES

1. Patel YC: Somatostatin and its receptor family. *Front Neuroendocrinol* 20:157–198, 1999
2. Vora JP, Owens DR, Ryder R, *et al*: Effect of somatostatin on renal function. *Br Med J (Clin Res Ed)* 292:1701–1702, 1986
3. Tulassay T, Tulassay Z, Rascher W, *et al*: Effect of somatostatin on kidney function and vasoactive hormone systems in health subjects. *Klin Wochenschr* 69:486–490, 1991
4. Schmidt A, Pleiner J, Schaller G, *et al*: Renal hemodynamic effects of somatostatin are not related to inhibition of endogenous insulin release. *Kidney Int* 61:1788–1793, 2002
5. Ray C, Carney S, Morgan T, Gillies A: Somatostatin as a modulator of distal nephron water permeability. *Clin Sci (Lond)* 84:455–460, 1993
6. Walker BJ, Evans PA, Forsling ML, Nelstrop GA: Somatostatin and water excretion in man: An intrarenal action. *Clin Endocrinol (Oxf)* 23:169–174, 1985
7. Brautbar N, Levine BS, Coburn JW, Kleeman CR: Interaction of somatostatin with PTH and AVP: Renal effects. *Am J Physiol* 237:E428–E436, 1979
8. Turman MA, O'Dorisio MS, O'Dorisio TM, *et al*: Somatostatin expression in human renal cortex and mesangial cells. *Regul Pept* 68:15–21, 1997
9. Kurokawa K, Aponte GW, Fujibayashi S, Yamada T: Somatostatin-like immunoreactivity in the glomerulus of rat kidney. *Kidney Int* 24:754–757, 1983
10. Turman MA, Apple CA: Human proximal tubular epithelial cells express somatostatin: Regulation by growth factors and cAMP. *Am J Physiol* 274:F1095–F1101, 1998
11. Davies JA, Bard JB: The development of the kidney. *Curr Top Dev Biol* 39:245–301, 1998
12. Bates CM, Kegg H, Petrevski C, Grady S: Expression of somatostatin receptors 3, 4, and 5 in mouse kidney proximal tubules. *Kidney Int* 63:53–63, 2003
13. Srinivas S, Goldberg M, Watanabe T, *et al*: Expression of green fluorescent protein in the ureteric bud of transgenic mice: A new tool for the analysis of ureteric bud morphogenesis. *Dev Genet* 24:241–251, 1999
14. Furuta T, Mori T, Lee T, Kaneko T: Third group of neostriatofugal neurons: Neurokinin B-producing neurons that send axons predominantly to the substantia innominata. *J Comp Neurol* 426:279–296, 2000
15. Nielsen S, Agre P: The aquaporin family of water channels in kidney. *Kidney Int* 48:1057–1068, 1995
16. Cho E, Patterson L, Brookhiser W, *et al*: Differential expression and function of cadherin-6 during renal epithelium development. *Development* 125:803–812, 1998
17. Silva FG, Nadasdy T, Laszik Z: Immunohistochemical and lectin dissection of the human nephron in health and disease. *Arch Pathol Lab Med* 117:1233–1239, 1993
18. Wessel GM: Cortical granule-specific components are present within oocytes and accessory cells during sea urchin oogenesis. *J Histochem Cytochem* 37:1409–1420, 1989
19. Spier AD, de Lecea L: Cortistatin: A member of the somatostatin neuropeptide family with distinct physiological functions. *Brain Res Brain Res Rev* 33:228–241, 2000
20. Vince DG, Tbakhi A, Gaddipati A, *et al*: Quantitative comparison of immunohistochemical staining intensity in tissues fixed in formalin and Histochoice. *Anal Cell Pathol* 15:119–129, 1997
21. Schindler M, Humphrey PP, Emson PC: Somatostatin receptors in the central nervous system. *Prog Neurobiol* 50:9–47, 1996
22. Bates CM, Kegg H, Grady S: Expression of somatostatin receptors 1 and 2 in the adult mouse kidney. *Regul Pept* (in press) 2004
23. Bersani M, Thim L, Baldissera FG, Holst JJ: Prosomatostatin 1-64 is a major product of somatostatin gene expression in pancreas and gut. *J Biol Chem* 264:10633–10636, 1989
24. Cristiani R, Petrucci C, Dal Monte M, Bagnoli P: Somatostatin (SRIF) and SRIF receptors in the mouse retina. *Brain Res* 936:1–14, 2002
25. Hall GH, Turnbull LW, Richmond I, *et al*: Localisation of somatostatin and somatostatin receptors in benign and malignant ovarian tumours. *Br J Cancer* 87:86–90, 2002
26. Nilsson L, Bergstrom L, Meyersson G, *et al*: Somatostatinergic phenotype markers in the human neuroblastoma cell-line LA-N-2. *FEBS Lett* 372:88–92, 1995
27. de Herder WW, Lamberts SW: Somatostatin and somatostatin analogues: Diagnostic and therapeutic uses. *Curr Opin Oncol* 14:53–57, 2002
28. Fisher WE, Wu Y, Amaya F, Berger DH: Somatostatin receptor subtype 2 gene therapy inhibits pancreatic cancer in vitro. *J Surg Res* 105:58–64, 2002
29. Krantic S: Peptides as regulators of the immune system: emphasis on somatostatin. *Peptides* 21:1941–1964, 2000
30. Schneider A, Grosch G, Stange EF, Ditschuneit H: Influence of triamcinolone and somatostatin on morphometric parameters of cultured intestinal mucosa. *In Vitro Cell Dev Biol* 22:647–652, 1986
31. Lehy T, Dubrasquet M, Bonfils S: Effect of somatostatin on normal and gastric-stimulated cell proliferation in the gastric and intestinal mucosae of the rat. *Digestion* 19:99–109, 1979
32. Castell T, Gomez de Segura IA, Vazquez I, *et al*: Somatostatin blockade improves the proliferative response but not intestinal morphological growth after small bowel resection in rats. *Eur J Surg* 167:54–59, 2001